Hindawi
International Transactions on Electrical Energy Systems
Volume 2023, Article ID 6328119, 11 pages
https://doi.org/10.1155/2023/6328119

Research Article

Short-Term Power Prediction of Wind Power Generation System Based on Logistic Chaos Atom Search Optimization BP Neural Network

Yihan Zhang, Peng Li, Huixuan Li, Wenjing Zu, and Hongkai Zhang

State Grid Henan Economic Research Institute, Zhengzhou 450000, China

Correspondence should be addressed to Peng Li; lipeng_ac@outlook.com

Received 7 October 2022; Revised 5 November 2022; Accepted 25 November 2022; Published 17 March 2023

Academic Editor: Xueqian Fu

Wind power generation is the major approach to wind energy utilization. However, due to the volatility, intermittent, and controllability of wind power, it is difficult to control and scheduling of wind power, which brings challenges to the grid-connected operation and dispatch of wind power. Therefore, accurate power prediction of the wind power generation system is worthy of in-depth study. And this paper proposes a wind power prediction model based on logistic chaos atom search optimization (LCASO) optimized back-propagation (BP) neural network, aiming to achieve accurate and efficient power prediction. Moreover, this work utilizes data preprocessing to obtain more precise prediction results and related prediction evaluation indexes to quantificationally compare the effect of the proposed one with other prediction models based on GA-BP neural network and PSO-BP neural network. In contrast with the BP neural network, GA-BP neural network, and PSO-BP neural network, the simulation tests verify the comprehensive prediction performance and wider applicability of LCASO-BP neural network-based power prediction model.

1. Introduction

Under the background of global carbon neutrality, the process of energy structure transformation is accelerating [1, 2]. More and more countries take the initiative to introduce relevant preferential policies and measures [3] to encourage the development of the renewable energy industry, and the green energy industry has a bright future [4–6].

However, the inherent intermittency and instability of wind power seriously restrict the development of wind power [7]. Prediction of wind power can reduce the operating cost of the power system [8] and mitigate the adverse effects of wind power, thus improving the competitiveness of wind turbines [9].

Several physical models based on weather data have been developed for wind speed prediction and wind power forecasting [10]. Physical models typically use global weather measurement databases or atmospheric mesoscale models [11, 12], but they require large computational systems to achieve accurate results and are therefore more reliable for long-term forecasting.

In addition, neural networks and support vector machines are representative ML [5, 13] methods that can accurately describe the stochastic nature of wind [14] by establishing a nonlinear mapping between input and output through various learning rules [15]. In particular, NNs can be divided into traditional neural networks and deep learning [16]. Traditional neural networks may not be able to identify some complex features of wind [17], such as long-term dependence. Therefore, deep learning methods have been introduced in the field of wind power prediction [18]. Reference [19] proposed a short-term prediction method of wind power based on the grey correlation analysis and adaptive upgrading of Tianniu Optimization Extreme learning machine, so as to realize the correction of the error of wind power short-term prediction model and improve the prediction accuracy. Reference [20] proposes an improved Drosophila optimization algorithm, which takes anemometer sequence reconstruction parameters and least squares

support vector machine parameters as optimization objectives to establish a wind speed prediction model. Reference [21] uses a small-world optimization algorithm to optimize the support vector machine combined with grey model to build wind power prediction model. Compared with a single support vector machine, this model improves the accuracy of prediction results. In addition, reference [22] constructed a wind turbine monitoring index prediction model based on long short-term memory neural network and an improved fuzzy comprehensive evaluation method based on the dynamic deterioration degree of indicators, which effectively improve the prediction accuracy of ultra-short-term offshore wind power.

With the development of wind power forecasting techniques [23], hybrid forecasting methods have been used to achieve better forecasts [24]. Hybrid forecasting is the use of combined models to obtain the best performance [25]. The combined models can be physical and statistical models, with different time scales or different statistical models [26]. In addition, horizontal combination methods employ weight coefficient assignment strategies, while vertical hybrid methods employ different methods at different prediction stages [3], such as parameter selection, data preprocessing, and data postprocessing. In addition, new techniques such as spatial correlation forecasting [27], regional forecasting, and offshore forecasting, which have been developed in recent years, have also received wide attention [28].

Based on the above research, a more accurate and effective prediction of the output power of wind and photovoltaic power generation systems is important not only for optimizing equipment capacity and installed frequency regulation but also for grid dispatch and online optimization of the unit mix. In summary, it is worthwhile to study and analyze the power prediction model of wind power systems.

The contributions made in this paper are as follows:

(i) The back-propagation (BP) neural network prediction model based on logistic chaos atom search optimization (LCASO) optimization is proposed.

(ii) The wind power prediction model based on LCASO-BP neural network is designed and compared with BP neural network, GA-BP neural network, and PSO-BP neural network through simulation, which effectively verifies its comprehensive prediction performance and wide applicability.

The rest of this paper is organized as follows: Section 2 introduces the modeling of the wind power generation system. Section 3 introduces LCASO-BP neural network. Section 4 introduces the wind power prediction based on LCASO-BP neural network, including data preprocessing, evaluation criteria, simulation test design, and simulation result analysis. Section 5 is a detailed summary and analysis of this paper. Section 6 looks forward to the future research direction.

2. Modeling of Wind Power Generation System

2.1. Effect of Wind Speed. The wind turbine's wind turbine absorbs energy from the natural wind and converts it into wind energy [29, 30], which is expressed as follows:

$$P_v = \frac{1}{2}\rho V^3 \pi R^2 C_p, \tag{1}$$

where P_v is the wind power absorbed by the wind turbine (kW); ρ is the air density (kg/m^3); V is the wind speed at the hub height of the wind turbine (m/s); and R represents the radius of the wind turbine's sweeping surface (m).

However, in the actual operation of wind farms, given the changing air density and wind speed under actual conditions, the wind speed and wind power are in a complex nonlinear relationship with each other, which can be described by the following equation:

$$P(v) = \begin{cases} 0, & 0 \le v \le V_a, \\ P_v, & V_a \le v \le V_c, \\ P_r, & V_c \le v \le V_b, \\ 0, & v \ge V_c, \end{cases} \tag{2}$$

where V_a represents the cut-in wind speed of the wind turbine; V_c represents the rated wind speed; V_b represents the cut-out wind speed; and P_r represents the rated output power.

From equation (2), it can be found that wind farm wind power and wind speed in different intervals have different functions, wind speed below V_a and above V_b, wind turbine shutdown work, but no change in output power, wind speed between V_a and V_c will cause a significant change in output power, wind speed between V_c and V_b, the generator set normal work under P_r.

2.2. Effect of Wind Direction. The influence of the natural wind direction of a wind farm on the output power of a wind turbine includes the following two aspects.

Above all, in wind turbine operation, in order to make the wind turbine capture as much wind energy as possible, the yaw device of the wind turbine will adjust the position of the wind turbine according to the recorded data of the anemometer and wind vane, however, since most of the yaw devices are time-delayed, the wind turbine cannot effectively align with the incoming wind, which will make the output power of the wind turbine different at the same wind speed.

Secondly, the wake effect will vary with the wind direction. That is, after the wind turbines of the upwind wind turbines capture the wind energy, the natural wind speed gradually decreases, making the wind energy through the downwind wind turbines significantly lower, and the corresponding output power will also decrease. Therefore, in the field setting and arrangement of wind farms, wind turbines are usually spaced far apart in order to reduce the harm of the wake effect.

2.3. The Effect of Air Density. It is obvious that the size of air density also affects the amount of natural wind energy captured by the wind turbine [31]. In addition, the air density is also closely related to the external temperature, relative humidity, atmospheric pressure, and other factors, which can be described as follows:

$$\rho = 1.276\frac{(P - 0.378(h/100)P_b)}{(1 + 0.00366t)/1000}, \tag{3}$$

where t represents the wind farm ground temperature; h represents the relative humidity; P represents the atmospheric pressure; and P_b represents the saturated water vapor pressure. From the above equation, it can be obtained that the wind turbine output power and air density are directly proportional to each other in the case of the remaining factors being constant. However, in the actual wind power output prediction, the NWP data are generally integrated, plus the influence of temperature, air pressure, and relative humidity.

3. LCASO-BP Neural Network

3.1. Logistic Chaos. Chaos is an inherent randomness phenomenon in certain nonlinear systems. Its change is not random but seemingly random, and it has the following characteristics: initial value sensitivity, boundedness, ergodicity, internal randomness, positive Lyapunov exponent, etc. [32]. The generation methods of chaotic sequences mainly use the following chaotic chaos: Logistic mapping, Tent mapping, Henon mapping, Lorenz mapping, and segment-by-segment linear chaotic mapping [33].

Logistic chaos is a relatively simple mapping method in mathematical form, and empirical experiments show that its chaotic system has good security and stability. Therefore, Logistic is used in this study to carry out chaotic mapping for the optimal individuals in the population. In addition, compared with other systems that generate chaotic variables, Logistic mapping is simple to use and requires less calculation. Therefore, Logistic mapping will be used to generate chaotic phenomena in standard atomic groups. The iterative equation of traditional logistic mapping is as follows:

$$x_{n+1} = \mu x_n(1 - x_n), \tag{4}$$

where μ represents the control parameter, $\mu \in (0, 4]$ and x_n represents the n th chaotic variable, $x_n \in (0, 1), n = 0, 1, 2, \cdots i$, which is defined between 0 and 1 in the continuous field of real numbers.

Particularly, when $3.57 < \mu < 4$, the whole system is in a chaotic state, so it is necessary to select μ The closer of μ it is to 4, the better of the whole chaos system. However, considering the actual situation when initializing the population position of atoms for chaotic mapping, this study sets $\mu = 3.8$, which is more effective and convenient.

Because when $x_n \in (0, 1)$ and $x_n \notin (0.25, 0.5, 0.75)$, the system is in the chaotic region, a small change of the initial variable will cause great differences in the subsequent orbits.

$$C_{n,j} = \frac{\left(x_{n,j} - b_{n,j}\right)}{\left(v_{n,j} - b_{n,j}\right)},$$
$$x_{n+1,j} = b_{n,j} + C_{n+1,j}\left(v_{n,j} - b_{n,j}\right), \tag{5}$$

where $C_{n,j}$ denotes the initial value of the chaotic sequence; j represents the dimension of the decision variable; and v_n and b_n represents the upper and lower limits of the initial decision variables, respectively.

In this way, the whole atomic group can use the global ergodic property of chaotic variables to optimize all solution spaces without falling into local extreme points. The general flow chart of Logistic chaotic mapping is shown in Figure 1.

3.2. BP Neural Network. BP neural networks consist of three layers: input, hidden, and output. Each layer consists of a certain number of neurons [34]. Each neuron has a threshold value and each level is connected by weights [35]. The relationship between the two levels of inputs and outputs can be considered as a mapping relationship, i.e., each set of inputs corresponds to a set of outputs, weights (or thresholds) are used to represent this relationship, and then the problem processing is performed.

In BP neural network, all layers except the input layer are composed of neurons, each of which is equivalent to a perceptron. The artificial neuron contains several parts, firstly, the input variable $x = (x_1, x_2, \ldots, x_m)$. Then is the threshold vector of the i-th neuron corresponding to the input variable $\omega = (\omega_{1j}, \omega_{2j}, \ldots, \omega_{mj})$. The neuron threshold is θ_j, the bias value of the neuron is b, the activation function is f, and the corresponding output value of the neuron is y_i. The correspondence between neuronal input and output is as follows:

$$y_i = f\left(\sum_{i=1}^{m} \omega_{ij}x_m + b\right). \tag{6}$$

The typical construction of a common three-layer BP neural network is shown in Figure 2. The left side is the input node, the right side is the output node, and the middle is the hidden layer.

The two phases of BP network learning are the forward scaling of the input signal and the backward scaling of the mistake. In the first stage, the training sample information is input to the input layer, then the hidden layer process it, and then passed it to the output layer. If there is a real output there is an error between the actual output and the predicted output, the second process is implemented. The second process is to pass the error of the output signal through the original path from the hidden layer to the input layer. Then, according to the assigned error signal, each neuron in each layer adjusts the connection of each network's weights and thresholds, last, the error signal is gradually reduced. These two processes are repeated alternately until the algorithm converges and satisfactory error accuracy is obtained.

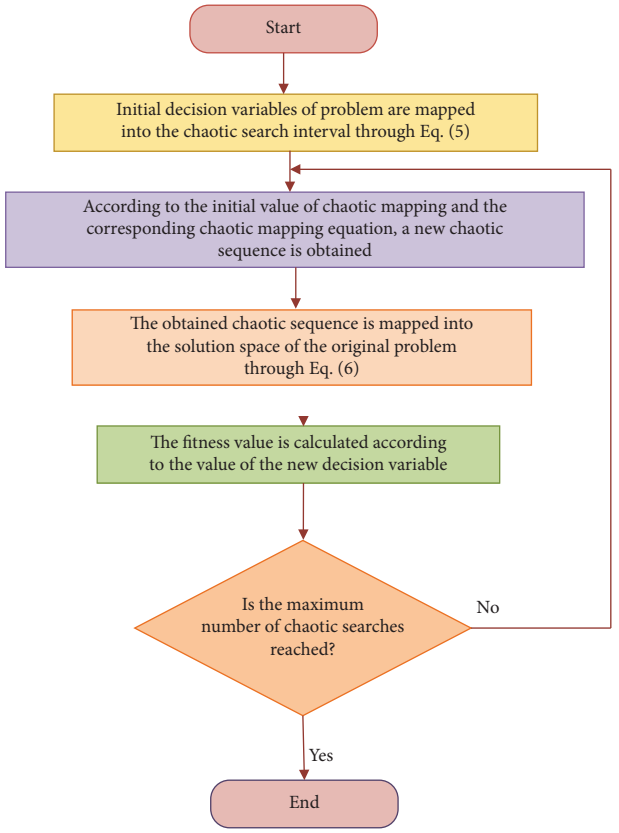

Figure 1: General flow chart of logistic chaotic.

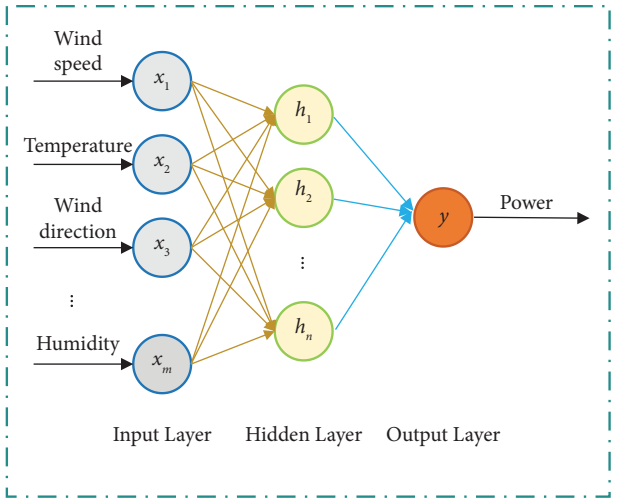

Figure 2: Basic structure of BP neural network.

3.3. Improved ASO Based on Logistic Chaos. The original ASO algorithm has a simple design and good applicability. However, it has the following two main defects: premature convergence and easy to fall into local optimization. Premature convergence will affect the exploration operation, that is, the global search ability, and falling into local optimization will affect the mining operation, that is, the local search ability. Therefore, the improved method designed in this study aims to balance the exploration and mining process in the optimization process of the original ASO. Based on this idea, this study introduces the logistic chaos theory into ASO (LCASO). By initializing the population position of atoms, the population individual with the best fitness is selected as the initial population, which further improves the quality of the initial atomic population solution and the efficiency of the algorithm. The optimization principle of LCASO is to add the logistic chaotic strategy to the group optimal value obtained by the optimization of ASO. Figure 3 is the flowchart of the LCASO algorithm.

4. Wind Power Prediction Based on LCASO-BP Network

4.1. Data Preprocessing. Generally speaking, there are two sources that affect the quality of input data samples. First, the input data samples have quality problems such as abnormal and missing values. Second, the magnitude and dimension of input data samples vary greatly. Common data sample problems can be roughly divided into three categories: integrity, accuracy, and effectiveness. In view of these problems, this section makes a simple cause analysis and expounds on the relevant detection standards. Among them, the detection standards of wind power data can refer to GB/T 18710-2002 standard [36].

First, the data integrity test. Incomplete data refer to the lack of a data value and some important attributes. The reason may be that the collection equipment has system failure and human operation error during data collection, or different factors are considered in data collection and data component analysis, as well as problems in data storage. The data integrity test can be carried out according to the following formula:

$$C_{\text{data}} = \frac{N_{\text{data}} - N_{\text{miss}}}{N_{\text{data}}} \times 100\%, \tag{7}$$

where C_{data} represents the integrity rate of wind measurement data; N_{data} indicates the number of data points that should be tested; and N_{miss} is expressed as the number of data points missing the test.

4.2. Evaluation Criteria. At present, there is no unified and specified evaluation standard to evaluate the prediction model. Some of the most commonly used evaluation indicators are mean absolute error (MAE), mean square error (MSE), mean absolute percentage error (MAPE), and root mean square error (RMSE). These four evaluation indexes can be expressed by the following formula:

$$\begin{aligned} MAE &= \frac{1}{n}\sum_{i=1}^{n}|x_i - y_i|, \\ \text{MSE} &= \frac{1}{n}\sum_{i=1}^{n}(x_i - y_i)^2, \\ \text{MAPE} &= \frac{1}{n}\sum_{i=1}^{n}\frac{|x_i - y_i|}{y_i} \times 100\%, \\ \text{RMSE} &= \sqrt{\frac{1}{n}\sum_{i=1}^{n}(x_i - y_i)^2}, \end{aligned} \tag{8}$$

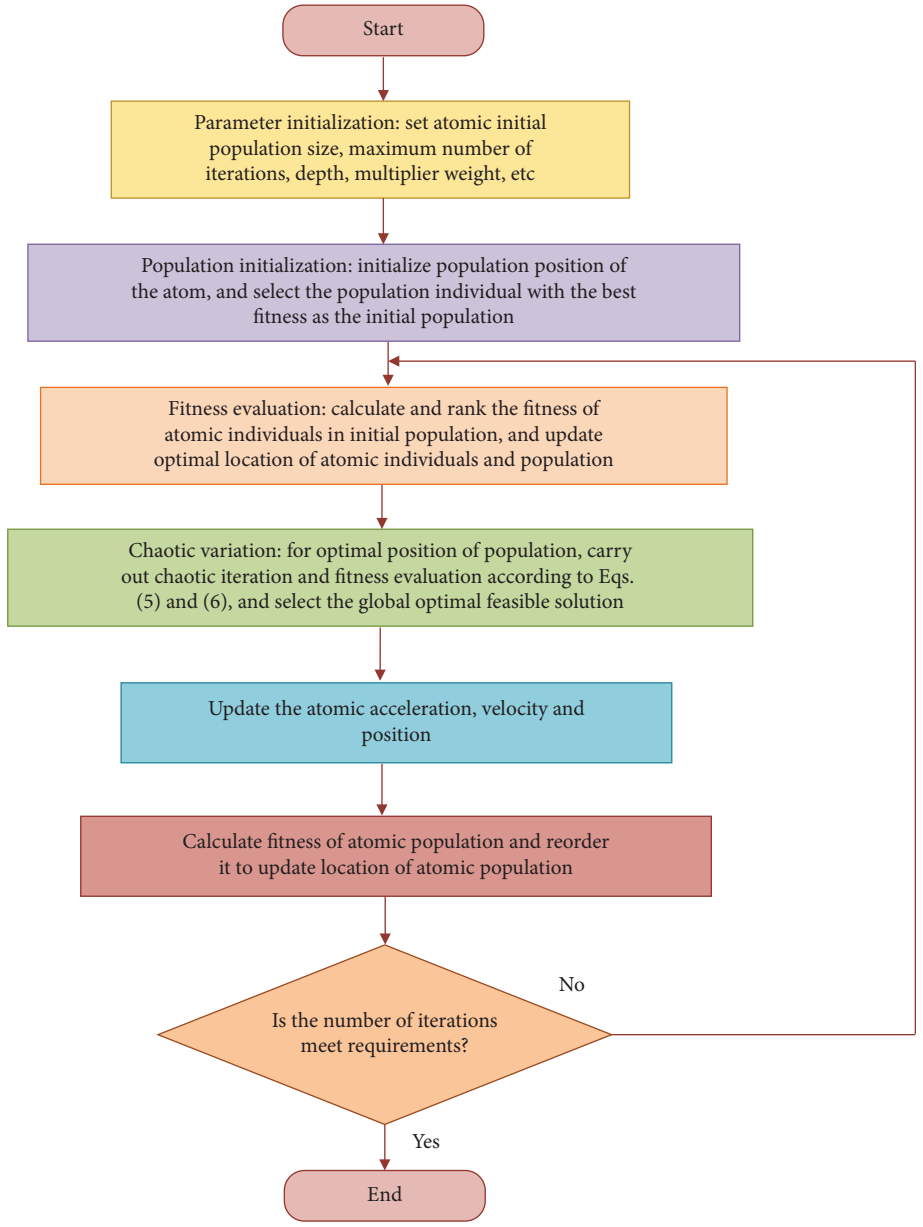

Figure 3: Flowchart of the LCASO algorithm.

where n is the number of prediction points and x_i and y_i is the predicted value and actual value, respectively.

4.3. Simulation Test Design. This section aims to apply LCASO-BP neural network to wind power system power, and to further verify the comprehensive performance of its prediction model, standard BP neural network, GA-BP neural network, and PSO-BP neural network are selected as comparison models for comparative simulation tests. The specific design process is as follows:

In the first step, a 2017 historical data set of a wind power station located in Ma Huang Mountain is firstly imported as the input dataset, followed by a series of preprocessing of the dataset so as to improve the quality of the input dataset, followed by dividing the training set into 27990 datasets and the test set into 50 datasets, and then linear normalization is performed on the input dataset. The simulation experiment is carried out on a personal computer based on MATLAB 2019b platform, in which the sampling time of MATLAB platform is 0.01 seconds, the solver is ode 45, and the computer uses Intel(R) Core TM i7-8650U CPU.

The second step is to determine the parameter settings of BP neural network and LCASO algorithm and comparison algorithm. The parameters of BP neural network are set as follows: the number of training times is 1000, the learning efficiency is set to 0.1, the network target accuracy is 0.1%, and the momentum coefficient is 0.8; the parameters of LCASO algorithm are set as follows: the initial population size is 30, the maximum number of iterations is 50, and the upper and lower limits of independent variables are (1, 3)

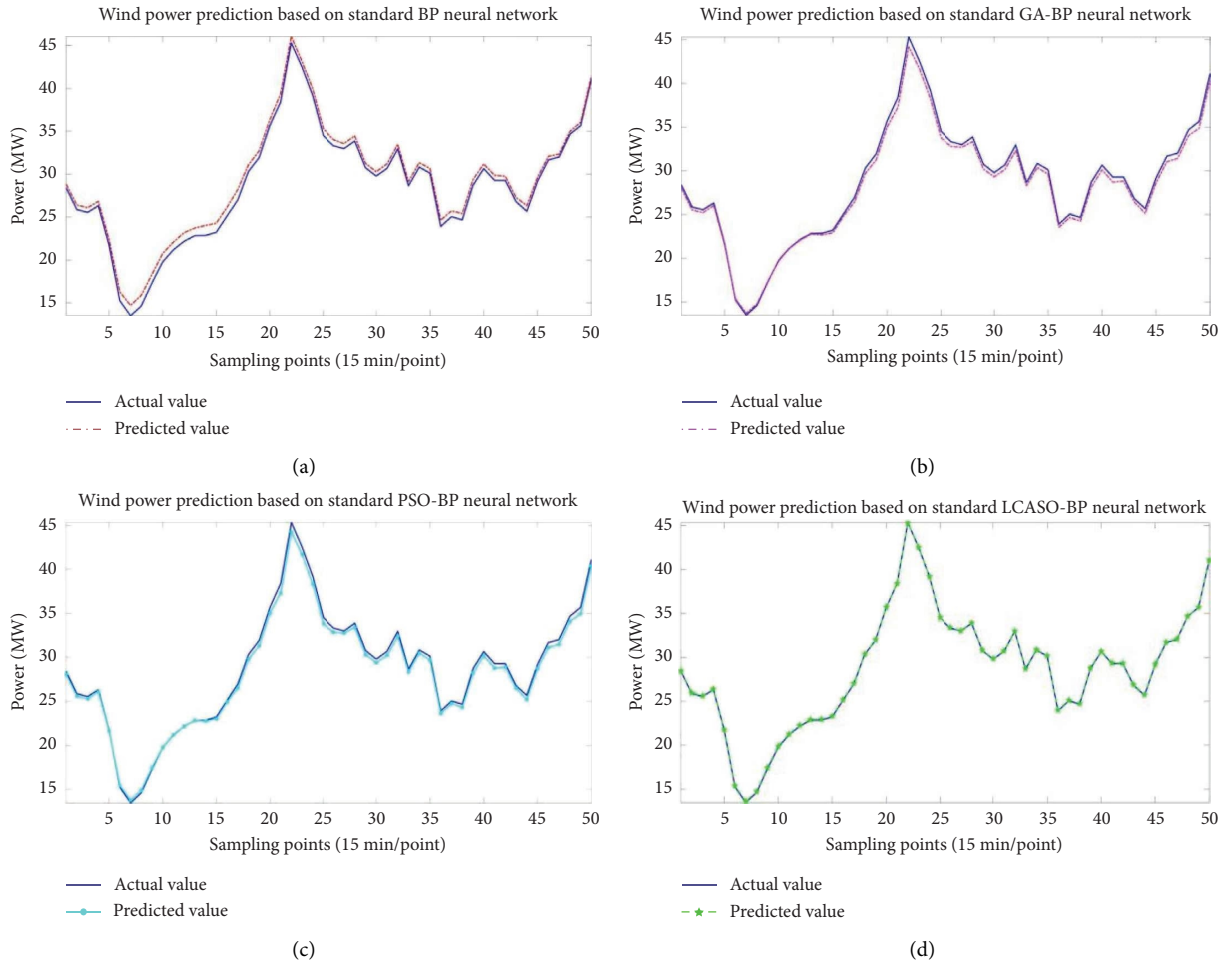

Figure 4: Wind power prediction curve based on (a) standard BP neural network; (b) GA-BP neural network; (c) PSO-BP neural network; (d) LCASO-BP neural network.

and (−3, 1), the depth and multiplier weights are 50 and 0.2, respectively.

In the third step, the optimal number of neuron nodes in the hidden layer of the three prediction models was determined as 9 by the experimental method and empirical formula method, and the input variables were wind speed (m/s) at 70 m of the wind measurement tower, wind direction (degree) at 70 m of the wind measurement tower, temperature (°C), air pressure (hPa), and humidity (%), and the output variable was the predicted output power (kW), and the input and output variables could be determined based on the input and output variables. The neuron nodes in the input and output layers are 5 and 1, respectively, so the structure of all three prediction models is a three-layer network structure with 5-9-1. In particular, to reduce the effect of random initialization on the overall prediction results, the average value of 20 independent experimental results is used for all the simulation test error evaluation index values in this section.

4.4. Simulation Results Analysis. The wind power prediction curves of BP neural network, GA-BP neural network, PSO-BP neural network, and LCASO-BP neural network are shown in Figures 4(a)–4(d). The comparison shows that the LCASO-BP neural network has the best prediction fit, compared to the GA-BP and PSO-BP neural networks, which have the second worst prediction fit and the BP neural network is the worst. This indicates that the trend of the power prediction of the BP neural network after LCASO optimization conforms to the actual power trend to a great extent. In addition, the comparison between the predicted power and the actual power in Figure 5 shows that the predicted power of the preoptimized BP neural network model, which can over- or lag to the peak, has been greatly improved, while the prediction accuracy of the three models after optimization has been improved to a certain extent, especially the predicted power curve of the LCAS-BP neural network basically matches the actual output power curve, which has a good understanding of the short-term power trend of the wind power system. The power trend of the wind power system has been well presented.

Figures 6 and 7 show the comparison of the four prediction models in terms of wind power prediction error indicators. It is easy to find that compared with the other three prediction models, the LCASO-BP neural network is much smaller in terms of AE and RE indicators, which indicates its better prediction effect and more stable

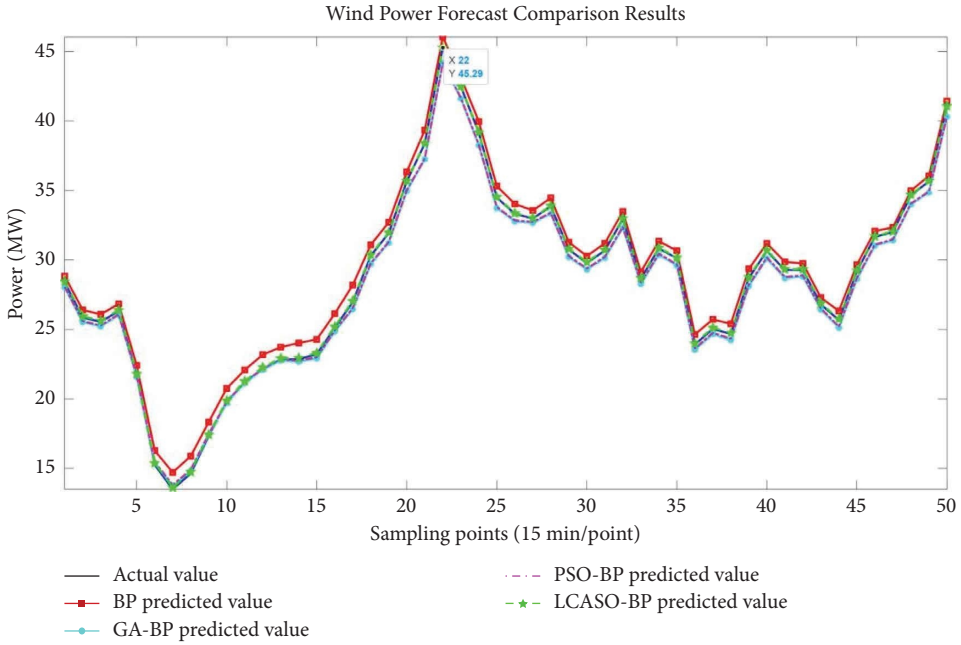

Figure 5: Results of wind power prediction versus actual value.

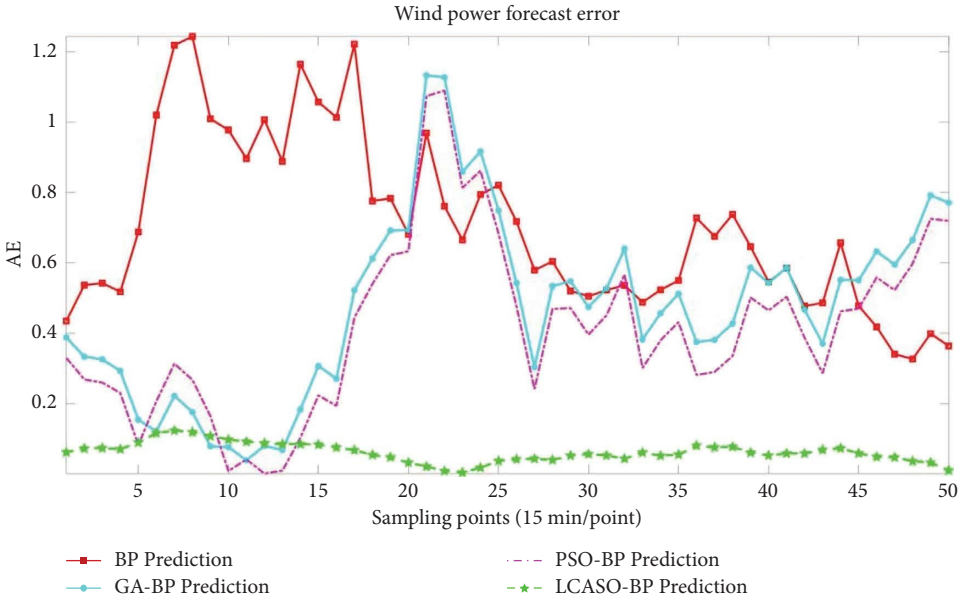

Figure 6: Comparison results of wind power prediction error AE.

prediction results. In addition, Table 1 shows the prediction and error values of the four prediction models at each of the five sampling points, and the table shows that the AE and RE values of the LCASO-BP neural network are the smallest at most of the sampling points, especially the RE value, which verifies the superior prediction performance of the LCASO-BP neural network model.

And Table 2 shows the results of the error evaluation metrics of the four prediction models. Compared with the other three prediction models, the LCASO-BP neural network has the smallest error evaluation metrics of MAE, MSE, RMSE, and MAPE, followed by the PSO-BP neural network. Among them, the MSE value of LCASO-BP is only 0.80% of the MAPE value in BP, and its MAPE, RMSE, and MAE values are only 9.12%, 0.80%, 8.96%, and 8.66% of the values in BP. It is noteworthy that the validation test of the comprehensive prediction ability of the relevant prediction models is more effective and accurate due to the significant increase of the input data sample size and the number of network training in this section, while the MSE, RMSE, MAE, and MAPE values in LCASO-BP are only 1.89%, 13.82%, 14.65%, and 18.65% of those in PSO-BP compared with the prediction model after PSO-optimized BP neural network, 14.65% and 18.54%, which further indicates that

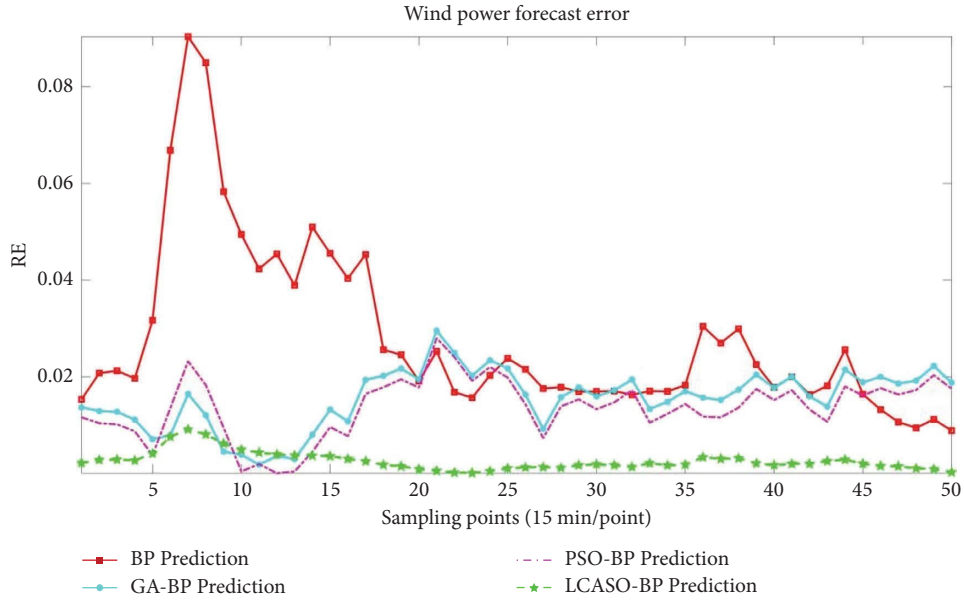

Figure 7: Wind power prediction error RE comparison results.

Table 1: Results of power prediction values for the four prediction models.

Sampling points	5	10	15	20	25	30	35	40	45	50
Measured values	21.7242	19.7778	23.2253	35.6639	34.5001	29.7842	30.1208	30.6493	29.1846	41.0771
BP predicted values	22.4122	20.7560	24.2829	36.3452	35.3211	30.2889	30.6706	31.1948	29.6624	41.4405
GA-BP predicted values	21.5707	19.7018	22.9188	34.9702	33.7510	29.3096	29.6088	30.1063	28.6340	40.3058
PSO-BP predicted values	21.6433	19.7858	23.0024	35.0307	33.8162	29.3884	29.6889	30.1845	28.7146	40.3577
LCASO-BP predicted values	21.8132	19.8748	23.3081	35.6955	34.5366	29.8400	30.1753	30.7016	29.2429	41.0865
AE values of BP	0.6880	0.9782	1.0576	0.6813	0.8209	0.5048	0.5498	0.5454	0.4778	0.3634
AE values of GA-BP	0.1535	0.0760	0.3065	0.6936	0.7490	0.4746	0.5120	0.5430	0.5505	0.7712
AE values of PSO-BP	0.0809	0.0080	0.2228	0.6331	0.6838	0.3958	0.4319	0.4648	0.4700	0.7194
AE values of LCASO-BP	0.0889	0.0969	0.0827	0.0316	0.0364	0.0558	0.0545	0.0522	0.0583	0.0094
RE values of BP	0.0316	0.0494	0.0455	0.0191	0.0238	0.0169	0.0183	0.0178	0.0163	0.0088
RE values of GA-BP	0.0070	0.0038	0.0132	0.0194	0.0217	0.0159	0.0170	0.0177	0.0188	0.0187
RE values of PSO-BP	0.0037	0.0004	0.0096	0.0177	0.0198	0.0133	0.0143	0.0151	0.0161	0.0175
RE values of LCASO-BP	0.0040	0.0049	0.0035	0.0008	0.0010	0.0019	0.0018	0.0017	0.0020	0.0002

Table 2: Error evaluation results of four prediction models.

Error assessment metrics	BP neural network	GA-BP neural network	PSO-BP neural network	LCASO-BP neural network
MSE	0.5526	0.2886	0.2323	0.0044
RMSE	0.7434	0.5373	0.4820	0.0666
MAE	0.7020	0.4726	0.4149	0.0608
MAPE	2.7839%	1.5495%	1.3699%	0.2540%

the prediction accuracy after optimization of BP neural network by LCASO algorithm is the most accurate among the four prediction models, and its comprehensive prediction performance and applicability are also the strongest.

In summary, the LCASO-BP neural network obtained the best prediction performance in the comparative simulation experiments of wind power prediction. On the one hand, the LCASO-BP neural network prediction model not only has some enhancement and improvement in overall stability and convergence speed compared with the other three prediction models, which indicates that the LCASO algorithm can be generally applied to the improvement of BP neural network in engineering practice. On the other hand, the LCAO-BP neural network prediction model obtains the smallest error and the best fitting accuracy, and it can be seen that the BP neural network improved by LCASO algorithm greatly improves the comprehensive prediction performance, which also verifies that the LCASO algorithm can better optimize the weights and thresholds of the BP neural network.

5. Conclusion

The development and utilization of increasingly popular new energy sources have been the focus of attention of researchers in the engineering field, and wind power generation has been widely used due to its advantages such as nonpollution and sustainability, but because wind power generation is difficult to predict, control, and dispatch, it poses a large hidden danger to the safety and grid stability. Furthermore, most of the current research is focused on wind power prediction, and the research horizon is not broad enough. To predict the power of wind power system more accurately, so as to reduce the errors of generation and consumption and ensure safety, reliable, and economic operation of power system, this study creatively designs and implements a wind power prediction model based on LCASO-BP neural network, which can effectively predict the future wind power.

The main contents and conclusions of this paper are briefly summarized as follows:

(1) A detailed introduction of the research background and significance of wind power system power prediction, and a detailed analysis and summary of the wind power characteristics analysis and its power prediction technology, provide a sufficient theoretical basis and rationale for the overall construction of the wind power system power prediction model.

(2) The BP neural network model based on LCASO optimization is elaborated. First, the ASO algorithm based on logistic chaos mapping is introduced in detail, and simulation tests and analysis are conducted to determine its feasibility and effectiveness. Then the principles of BP neural network and its shortcomings are analyzed, based on which a BP neural network prediction model based on LCASO optimization is proposed, and its prediction performance and generality are verified through simulation tests.

(3) A detailed analysis of the data preprocessing process and relevant prediction evaluation indexes of wind power generation systems is presented, and power prediction models based on GA-BP neural networks and PSO-BP neural networks are established and simulated and tested to provide effective and scientific references for subsequent comparative simulation experiments.

(4) Based on the previous research and analysis, the wind power prediction model based on LCASO-BP neural network is designed and its comprehensive prediction performance and wide applicability are effectively verified through comparative simulation tests with BP neural network, GA-BP neural network, and PSO-BP neural network, respectively. The simulation results show that the LCASO-BP neural network prediction model has excellent prediction accuracy and fitting effect, and has significant advantages in overall stability and convergence.

6. Prospect

In the course of this research, a short-term power prediction model for wind power generation system based on LCASO-BP neural network has been designed, but there are still some future works in this subject area that need to be studied and solved in depth, mainly in the following aspects:

(1) *Prediction Time Scale*. In this study, several short-term prediction models based on improved BP neural networks have been designed for wind power generation systems, but the feasibility and effectiveness of BP neural networks and their improved models for medium and long-term power prediction of wind power generation systems have not been studied in depth.

(2) *Prediction Spatial Scale*. In this study, only the resource data related to a single wind power plant at a location in Ma Huang Mountain are used as the research object.

(3) In practice, many wind farms appear to be clustered and scaled, so future research can focus on the power prediction of the entire wind farm cluster area.

(4) *Prediction Algorithm Model*. This study only applies the heuristic algorithm and its improvement algorithm to optimize the BP neural network model in the wind power system power prediction and does not further research and analysis on other advanced models, and innovative research on prediction models can be conducted in the future, such as machine learning algorithms and hybrid artificial intelligence algorithms.

(5) *Input Data Preprocessing*. This study only uses common data preprocessing methods to examine and process the input dataset, which has certain uncertainties and limitations, and other input data preprocessing mechanisms, such as principal component analysis, feature selection methods, and methods based on cluster analysis, can be further investigated in the future.

(6) *Power Uncertainty Analysis*. As the power prediction of wind power generation system is inherently uncertain, accurate analysis of its power prediction uncertainty is the key to ensure grid dispatch and safe and stable operation. The power uncertainty analysis can be roughly divided into parametric and nonparametric methods according to the modeling framework, which can be analyzed qualitatively and quantitatively in the future.

Data Availability

The wind power data used to support the findings of this study were supplied by State Grid Corporation of China under license and so cannot be made freely available. Requests for access to these data should be made to Peng Li, lipeng_ac@outlook.com.

Conflicts of Interest

Authors Yihan Zhang, Peng Li, Huixuan Li, Wenjing Zu, and Hongkai Zhang are all employed by State Grid Henan Economic Research Institute. All the authors declare that the research was conducted in the absence of any commercial or financial relationships that could be construed as a potential conflicts of interest.

Acknowledgments

This work was supported by the State Grid Corporation of China (1400-202224249A-1-1-ZN).

References

[1] B. Yang, L. Zhong, J. Wang et al., "State-of-the-art one-stop handbook on wind forecasting technologies: an overview of classifications, methodologies, and analysis," *Journal of Cleaner Production*, vol. 283, Article ID 124628, 2021.

[2] X. Q. Fu and H. Niu, "Key technologies and applications of agricultural energy internet for agricultural planting and fisheries industry," *Information Processing in Agriculture*, 2022.

[3] J. Jung and R. P. Broadwater, "Current status and future advances for wind speed and power forecasting," *Renewable and Sustainable Energy Reviews*, vol. 31, pp. 762–777, 2014.

[4] F. Ji, X. Cai, and J. Wang, "Wind power correlation analysis based on hybrid copula," *Automation of Electric Power Systems*, vol. 2, pp. 1–5, 2014.

[5] X. Q. Fu, Q. L. Guo, and H. B. Sun, "Statistical machine learning model for stochastic optimal planning of distribution networks considering a dynamic correlation and dimension reduction," *IEEE Transactions on Smart Grid*, vol. 11, no. 4, pp. 2904–2917, 2020.

[6] X. Q. Fu, "Statistical machine learning model for capacitor planning considering uncertainties in photovoltaic power," *Protection and Control of Modern Power Systems*, vol. 7, no. 1, 2022.

[7] H. A. Kazem and J. H. Yousif, "Comparison of prediction methods of photovoltaic power system production using a measured dataset," *Energy Conversion and Management*, vol. 148, pp. 1070–1081, 2017.

[8] D. Song, J. Yang, X. Fan et al., "Maximum power extraction for wind turbines through a novel yaw control solution using predicted wind directions," *Energy Conversion and Management*, vol. 157, pp. 587–599, 2018.

[9] P. K. Guchhait and A. Banerjee, "Stability enhancement of wind energy integrated hybrid system with the help of static synchronous compensator and symbiosis organisms search algorithm," *Protection and Control of Modern Power Systems*, vol. 5, no. 1, pp. 11–150, 2020.

[10] J. Wang, Y. Song, F. Liu, and R. Hou, "Analysis and application of forecasting models in wind power integration: a review of multi-step-ahead wind speed forecasting models," *Renewable and Sustainable Energy Reviews*, vol. 60, pp. 960–981, 2016.

[11] E. Erdem and J. Shi, "ARMA based approaches for forecasting the tuple of wind speed and direction," *Applied Energy*, vol. 88, no. 4, pp. 1405–1414, 2011.

[12] D. Ambach and W. Schmid, "A new high-dimensional time series approach for wind speed, wind direction and air pressure forecasting," *Energy*, vol. 135, pp. 833–850, 2017.

[13] D. Liu, D. Niu, H. Wang, and L. Fan, "Short-term wind speed forecasting using wavelet transform and support vector machines optimized by genetic algorithm," *Renewable Energy*, vol. 62, pp. 592–597, 2014.

[14] X. Fu, "Statistical machine learning model for capacitor planning considering uncertainties in photovoltaic power," *Protection and Control of Modern Power Systems*, vol. 7, pp. 5–63, 2022.

[15] S. N. N. H. Binti, K. H. Chong, C. T. Yaw, and S. P. Koh, *Application of Machine Learning Technique Using Support Vector Machine in Wind Turbine Fault Diagnosis*, Queensland University of Technology, Brisbane City, Australia, 2014.

[16] H. Raju and S. Das, "CNN-based deep learning model for solar wind forecasting," *Solar Physics*, vol. 296, pp. 134–139, 2021.

[17] M. Jaume, B. Javier, and C. Ulises, ""Dust in the wind…", deep learning application to wind energy time series forecasting," *Energies*, vol. 12, 2019.

[18] A. Saeed, C. S. Li, M. Danish et al., "Hybrid bidirectional LSTM model for short-term wind speed interval prediction," *IEEE Access*, vol. 8, pp. 182283–182294, 2020.

[19] J. H. Ye, X. Wei, D. Q. Huang, L. Xei, C. Huang, and S. Zhao, "Short-term forecast of wind power based on bso-elm-adaboost with grey correlation analysis," *Acta Energiae Solaris Sinica*, vol. 43, no. 3, pp. 426–432, 2022.

[20] Q. M. Cheng, L. Chen, and Y. M. Cheng, "Short-term wind power forecasting method based on EEMD and LS-SVM model," *Electric Power Automation Equipment*, vol. 38, no. 5, pp. 27–35, 2018.

[21] S. X. Wang, X. Zhao, and T. Li, "Wind power variable weight combination forecasting model based on small world optimization," *Acta Energiae Solaris Sinica*, vol. 36, no. 12, pp. 2867–2873, 2015.

[22] L. L. Huang, S. Li, Y. Fu, and L. Wang, "Ultra-short term offshore wind power prediction based on condition-assessment of wind turbines," *Acta Energiae Solaris Sinica*, vol. 43, no. 8, pp. 391–398, 2022.

[23] H. Liu, H. Q Tian, C. Chen, and Y. F. Li, "An experimental investigation of two wavelet-MLP hybrid frameworks for wind speed prediction using GA and PSO optimization," *International Journal of Electrical Power & Energy Systems*, vol. 52, pp. 161–173, 2013.

[24] T. Liang, C. Y. Chen, C. X. Mei, Y. Jing, and H. Sun, "A wind speed combination forecasting method based on multifaceted feature fusion and transfer learning for centralized control center," *Electric Power Systems Research*, vol. 213, Article ID 108765, 2022.

[25] Z. Liang, J. Liang, L. Zhang, C. Wang, Z. Yun, and X. Zhang, "Analysis of multi-scale chaotic characteristics of wind power based on Hilbert-Huang transform and Hurst analysis," *Applied Energy*, vol. 159, pp. 51–61, 2015.

[26] N. Stevesonn, M. Mesbah, and B. Boashash, "A sampling limit for the empirical mode decomposition," in *Proceedings of the Signal Processing and its Applications*, pp. 647–650, August 2005, Sydeny, Australia.

[27] L. V. Bremen, N. Saleck, and D. Heinemann, "Enhanced regional forecasting considering single wind farm distribution for upscaling," *Journal of Physics: Conference Series*, vol. 75, p. 012040, 2007.

[28] S. Wang, N. Zhang, L. Wu, and Y. Wang, "Wind speed forecasting based on the hybrid ensemble empirical mode decomposition and GA-BP neural network method," *Renewable Energy*, vol. 94, pp. 629–636, 2016.

[29] Y. L. Li, K. Wang, Z. D. Gao, D. Wang, N. Song, and Q. Zhu, "Research on modification method of voltage control area considering wind power connection," *Acta Energiae Solaris Sinica*, vol. 43, no. 9, pp. 258–266, 2022.

[30] J. H. Yang, J. H. Zheng, and H. X. Feng, "Doubly-fed variable speed wind generation system using matrix converter," *High Voltage Engineering*, vol. 35, no. 11, pp. 2820–2825, 2009.

[31] F. L. Yang, H. J. Zhang, and S. Shao, "Field observation of air density for transmission line corridors in high-altitude regions," *Electric power*, vol. 54, no. 12, pp. 170–176, 2021.

[32] S. Sahoo and B. K. Roy, "Design of multi-wing chaotic systems with higher largest Lyapunov exponent," *Chaos, Solitons & Fractals*, vol. 157, Article ID 111926, 2022.

[33] D. T. Que, N. X. Quyen, and T. M. Hoang, "Performance of Improved-DCSK system over land mobile satellite channel under effect of time-reversed chaotic sequences," *Physical Communication*, vol. 47, Article ID 101342, 2021.

[34] J. B. Zhou, K. Wang, G. Yang, X. Liu, R. Du, and Y. Li, "Real-time uncertainty estimation of stripe center extraction results using adaptive BP neural network," *Measurement*, vol. 194, no. 15, Article ID 111022, 2022.

[35] E. Mahidin, "A critical review of the integration of renewable energy sources with various technologies," *Protection and Control of Modern Power Systems*, vol. 6, no. 1, pp. 3–54, 2021.

[36] Z. X. Liu, G. S. Du, S. A. Zhou, H. Lu, and H. Ji, "Analysis of internet financial risks based on deep learning and BP neural network," *Computational Economics*, vol. 59, no. 4, pp. 1481–1499, 2022.